Inorg. Chem. **2005**, *44*, 709–715

Synthesis, Crystal Structure, and Magnetic Properties of Oxime-Bridged Polynuclear Ni(II) and Cu(II) Complexes

Yun-Bo Jiang,[†] Hui-Zhong Kou,*[,†] Ru-Ji Wang,[†] Ai-Li Cui,[†] and Joan Ribas[‡]

Department of Chemistry, Tsinghua University, Beijing 100084, P. R. China and Departament de Química Inorgànica, Universitat de Barcelona, Diagonal 6487, 08028-Barcelona, Spain

Received September 10, 2004

Two new polynuclear complexes $[Ni_6(amox)_6(\mu_6\text{-}O)(\mu_3\text{-}OH)_2]Cl_2\cdot 6H_2O$ and $[Cu_3(amox)_3(\mu_3\text{-}OH)(\mu_3\text{-}Cl)]ClO_4\cdot 4H_2O$ ($amox^- =$ anion of 4-amino-4-methyl-2-pentanone oxime) have been synthesized and characterized structurally and magnetically. The Ni(II) complex contains a novel Chinese-lantern-like Ni_6 cage centered by an oxo ion. It contains the nearest octahedral Ni(II)···Ni(II) separation (<2.8 Å) and exhibits strong antiferromagnetic properties. The Cu(II) complex has a cyclic trinuclear copper(II) core bridged by both μ_3-OH^- and μ_3-Cl^- ions. The magnetic susceptibilities of both antiferromagnetic complexes were fitted by using approximate models.

Introduction

Magnetism of high-nuclearity complexes is currently an active field of research[1−11] since it was discovered that a Mn_{12} complex exhibits single-molecule magnet (SMM) behavior.[5] However, the synthesis of such species is challenging. Various synthetic methods have been developed, for example, self-assembly and the use of metalloligands.[6] The synthetic route is to carefully select the bridging ligands and control the hydrolysis or alcoholysis of metal ions in the presence of auxiliary ligands.[5,10]

It has been shown that the oxime ligands can connect two transition-metal ions, generating oxime-bridged polynuclear complexes. Also, the ability of the oxime group to efficiently transmit magnetic coupling has been well documented.[7−11] However, it is desirable to search for new oxime ligands to construct new oxime-bridged paramagnetic transition-metal complexes. Focusing on Ni(II) and Cu(II) ions, we have chosen amoxH[11,12] (amoxH = 4-amino-4-methyl-2-pentanone

* To whom correspondence should be addressed. E-mail: kouhz@mail.tsinghua.edu.cn.
† Tsinghua University.
‡ Universitat de Barcelona.

(1) (a) Tesmer, M.; Muller, B.; Vahrenkamp, H. *Chem. Commun*. **1997**, 721. (b) Röder, J. C.; Meyer, F.; Pritzkow, H. *Chem. Commun*. **2001**, 2176. (c) Shaw, R.; Tidmarsh, I. S.; Laye, R. H.; Breeze, B.; Helliwell, M.; Brechin, E. K.; Heath, S. L.; Murrie, M.; Ochsenbein, S.; Gudel, H.-U.; McInnes, E. J. L. *Chem. Commun*. **2004**, 1418.
(2) Campos-Fernandez, C. S.; Clerac, R.; Dunbar, K. R. *Angew. Chem., Int. Ed*. **1999**, *38*, 3477. Xu, Z.; Thompson, L. K.; Milway, V. A.; Zhao, L.; Kelly, T.; Miller, D. O. *Inorg. Chem*. **2003**, *42*, 2950.
(3) Serna, Z. E.; Lezama, L.; Urtiaga, M. K.; Arriortua, M. I.; Barandika, M. G.; Cortes, R.; Rojo, T. *Angew. Chem., Int. Ed*. **2000**, *39*, 344.
(4) Liu, X.; McAllister, J. A.; de Miranda, M. P.; Whiteker, B. J.; Kilner, C. A.; Thornton-Pett, M.; Halcrow, M. A. *Angew. Chem., Int. Ed*. **2002**, *41*, 756. Murugesu, M.; Clerac, R.; Anson, C.; Powell, A. K. *Chem. Commun*. **2004**, 1598.
(5) Sessoli, R.; Gatteschi, D.; Caneschi, A.; Novak, M. A. *Nature* **1993**, *365*, 141. Sessoli, R.; Tsai, H.-L.; Schake, A. R.; Wang, S.; Vincent, J. B.; Folting, K.; Gatteschi, D.; Christou, G.; Hendrickson, D. N. *J. Am. Chem. Soc*. **1993**, *115*, 1804. Winpenny, R. E. P. *Dalton Trans*. **2002**, 1. King, P.; Clerac, R.; Wernsdorfer, W.; Anson, C. E.; Powell, A. K. *Dalton Trans*. **2004**, 2670.
(6) Cotton, F. A.; Winquist, B. H. C. *Inorg. Chem*. **1969**, *8*, 1304. Bertrand, J. A.; Ginsberg, A. P.; Kaplan, R. I.; Kirkwood, C. E.; Martin, R. L.; Sherwood, R. C. *Inorg. Chem*. **1971**, *10*, 240. Brechin, E. K.; Gould, R. O.; Harris, S. G.; Parsons, S.; Winpenny, R. E. P. *J. Am. Chem. Soc*. **1996**, *118*, 11293. Clemente-Juan, J. M.; Chansou, B.; Donnadieu, B.; Tuchagues, J.-P. *Inorg. Chem.* **2000,** *39*, 5515. Moragues-Canovas, M.; Helliwell, M.; Ricard, L.; Riviere, E.; Wernsdorfer, W.; Brechin, E.; Mallah, T. *Eur. J. Inorg. Chem.* **2004**, 2219. Ochsenbein, S. T.; Murrie, M.; Rusanov, E.; Stoeckli-Evans, H.; Sekine, C.; Gudel, H. U. *Inorg. Chem*. **2002**, *41*, 5133.
(7) Milios, C. J.; Raptopoulou, C. P.; Terzis, A.; Lloret, F.; Vicente, R.; Perlepes, S. P.; Escuer, A. *Angew. Chem., Int. Ed*. **2004**, *43*, 210. Thorpe, J. M.; Beddoes, R. L.; Collison, D.; Garner, C. D.; Helliwell, M.; Holmes, J. M.; Tasker, P. A. *Angew. Chem., Int. Ed*. **1999**, *38*, 1119.
(8) Chaudhuri, P. *Coord. Chem. Rev*. **2003**, *243*, 143 and references therein.
(9) Psomas, G.; Dendrinou-Samara, C.; Alexiou, M.; Tsohos, A.; Raptopoulou, C. P.; Terzis, A.; Kessissoglou, D. P. *Inorg. Chem.* **1998**, *37*, 6556. Pavlishchuk, V. V.; Kolotilov, S. V.; Addison, A. W.; Prushan, M. J.; Butcher, R. J.; Thompson, L. K. *Inorg. Chem.* **1999**, *38*, 1759. Pavlishchuk, V.; Birkelbach, F.; Weyhermuller, T.; Wieghardt, K.; Chaudhuri, P. *Inorg. Chem.* **2002**, *41*, 4405. Psomas, G.; Stemmler, A. J.; Dendrinou-Samara, C.; Bodwin, J. J.; Schneider, M.; Alexiou, M.; Kampf, J. W.; Kessissoglou, D. P.; Pecoraro, V. L. *Inorg. Chem.* **2001**, *40*, 1562. Pavlishchuk, V. V.; Kolotilov, S. V.; Addison, A. W.; Prushan, M. J.; Schollmeyer, D.; Thompson, L. K.; Goreshnik, E. A. *Angew. Chem., Int. Ed*. **2001**, *40*, 4734.
(10) Afrati, T.; Dendrinou-Samara, C.; Raptopoulou, C. P.; Terzis, A.; Tangoulis, V.; Kessissoglou, D. P. *Angew. Chem., Int. Ed*. **2002**, *41*, 2148. Sreerama, S. G.; Pal, S. *Inorg. Chem*. **2002,** *41*, 4843.
(11) Curtis, N. F.; Gladkikh, O. P.; Heath, S. L.; Morgan, K. R. *Aust. J. Chem*. **2000**, *53*, 577.

10.1021/ic048729m CCC: $30.25 © 2005 American Chemical Society
Published on Web 01/05/2005

oxime) as the bridging ligand and successfully synthesized a new μ_3-OH^- and μ_3-Cl^- doubly bridged trinuclear Cu(II) complex and a novel hexanuclear cage that contains paramagnetic octahedral Ni^{II} ions. Cu(II)−$amox^-$ complexes have been reported by Curtis et al., including dinuclear and hydrogen-bonded hexanuclear ones.[12] A number of complexes with a $Cu_3O(H)$ core held by peripheral bridging ligands have been described so far.[13−16] Actually, only few of them containing both μ_3-OH^- and μ_3-Cl^- bridges have been reported in the literature to our knowledge.[16]

It is interesting to note that oxime-bridged Ni^{II} complexes have been rarely characterized magnetically and structurally, and consequently no definite magneto-structural relationship could be obtained.[8] A structurally similar ligand aoH (aoH = 2-amino-2-methyl-3-butanone oxime) reacts with Ni^{2+}, producing a monomer $[Ni(ao)_2-H]Cl\cdot H_2O$ that contains four-coordinate diamagnetic Ni^{II} ions.[17] In the present paper we describe the systematic studies on the $amox^-$ bridging ligands.

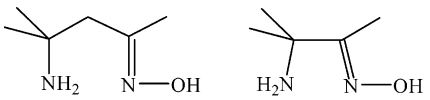

amoxH aoH

Experimental Section

Elemental analyses of carbon, hydrogen, and nitrogen were carried out with an Elementar Vario EL. Infrared spectroscopy was performed on a Magna-IR 750 spectrophotometer in the 4000−400 cm^{-1} region. Magnetic measurements were performed on a few manually separated single crystals using a MagLab 2000 magnetometer. The experimental susceptibilities were corrected for the diamagnetism of the constituent atoms (Pascal's Tables). The ligand amoxH was synthesized according to the literature method.[11]

Caution! Although not encountered in our experiments, perchlorate derivatives are potentially explosive. Only a small amount of the materials should be prepared, and it should be handled with care.

Synthesis of $[Ni_6(amox)_6(\mu_6\text{-}O)(\mu_3\text{-}OH)_2]Cl_2\cdot 6H_2O$ (1). Well-shaped block blue single crystals are first formed by slowly cooling a warm aqueous solution containing amoxH and $NiCl_2\cdot 6H_2O$ (molar ratio = 2:1) in low yield. Platelet blue single crystals could be deposited in higher yield by slow evaporation of a dilute aqueous solution at room temperature after a few weeks. The two materials of different crystal shapes are characterized to be identical. The method is reproducible. Yield: 50%. Anal. Calcd: C, 31.88; H, 6.84; N, 12.39. Found: C, 31.48; H, 6.86; N, 12.58. The complex is soluble in hot water and insoluble in common organic solvents. IR: ν = 1622, 1595 (C═N), 1036, 1198 (O−N) cm^{-1}.

Synthesis of $[Cu_3(amox)_3(\mu_3\text{-}OH)(\mu_3\text{-}Cl)]ClO_4\cdot 4H_2O$ (2). Copper(II) chloride tetrahydrate and amoxH were dissolved in a mixture of MeOH−H_2O (2:1, v/v). After leaving the solution undisturbed for 1 day, an excess amount of solid $NaClO_4$ was added to the solution. Slow evaporation of the resultant solution gave dark green crystals suitable for single-crystal X-ray diffraction analysis. They were collected manually. Yield: 40%. Anal. Calcd: C, 26.95; H, 6.03; N, 10.48. Found: C, 27.02; H, 6.05; N, 10.51. IR: ν = 1630, 1602 cm (C═N), 1058, 1211 (O−N) cm^{-1}.

X-ray Structure Determination. Data collection of **1** and **2** were made on a Bruker Smart CCD (293 K) diffractometer. The absorption corrections have been applied by using SADABS (Bruker 2000) for both complexes. The structures were solved by direct method SHELXS-97 and refined by full-matrix least squares (SHELXL-97) on F^2. Hydrogen atoms attached to the C and N atoms were added geometrically and refined using a riding model. The $amox^-$ ligands around the nickel atoms in **1** were disordered, and a split model was used during the refinement. The crystal data are summarized in Table 1.

Table 1. Crystal Data for Complexes **1** and **2**

	1	**2**
formula	$C_{36}H_{92}Cl_2N_{12}Ni_6O_{15}$	$C_{18}H_{48}Cl_2Cu_3N_6O_{12}$
fw	1356.38	802.14
space group	*C*2/*m*	*P*2(1)/*c*
a/Å	21.111(1)	12.611(3)
b/Å	13.1963(8)	21.931(4)
c/Å	11.8430(7)	11.987(2)
β/deg	116.385(1)	92.45(3)
V/Å^3	2955.65(52)	3312.2(11)
Z	2	4
ρ_{calcd}/g cm^{-3}	1.524	1.609
μ(Mo Kα)/mm^{-1}	2.028	2.130
data/restraint/params	2973/6/257	5814/0/370
GOF	1.055	1.064
R1 [$I > 2\sigma(I)$]	0.0488	0.0658
wR2 (all data)	0.1355	0.1091

Results and Discussion

Synthesis. The complex $[Ni_6(amox)_6(\mu_6\text{-}O)(\mu_3\text{-}OH)_2]Cl_2\cdot 6H_2O$ (**1**) is prepared by the self-assembly reaction of $NiCl_2\cdot 6H_2O$ and an excess amount of amoxH in aqueous solution. The formula of the complex was determined by microelemental analyses and single-crystal X-ray diffraction analysis. It should be noted that use of methanol as the reaction media generated an oily material. This further supports that the formation of the μ_6-O-centered Ni_6 cluster involves the hydrolysis reaction and self-assembly.

Spontaneous self-assembly of amoxH, $CuCl_2\cdot 4H_2O$, and $NaClO_4$ in a methanol−H_2O mixture solution gives trinuclear $[Cu_3(amox)_3(\mu_3\text{-}OH)(\mu_3\text{-}Cl)]ClO_4\cdot 4H_2O$ (**2**), whereas $\{[Cu_3(amox)_3O]_2H]\}(ClO_4)_3\cdot 3H_2O$ was obtained in the absence of Cl^- ions.[11]

Crystal Structures. Selected bond distances and angles for complexes **1** and **2** are listed in Tables 2 and 3,

(12) Morgan, K. R.; Curtis, N. F. *Aust. J. Chem.* **1980**, *33*, 1231.
(13) Gehring, S.; Fleischhauer, P.; Paulus, H.; Haase, W. *Inorg. Chem.* **1993**, *32*, 54. Clerac, R.; Cotton, F. A.; Dunbar, K. R.; Hillard, E. A.; Petrukhina, M. A.; Smucker, B. W. *C. R. Acad. Sci. Paris, Chimie/Chem.* **2001**, *4*, 315.
(14) Costes, J.-P.; Dahan, F.; Laurent, J.-P. *Inorg. Chem.* **1986**, *25*, 413. Ferrer, S.; Haasnoot, J. G.; Reedijk, J.; Muller, E.; Cingi, M. B.; Lanfranchi, M.; Lanfredi, A. M. M.; Ribas, J. *Inorg. Chem.* **2000**, *39*, 1859. Ferrer, S.; Lloret, F.; Bertomeu, I.; Alzuet, G.; Borras, J.; Garcia-Granda, S.; Liu-Gonzalez, M.; Haasnoot, J. G. *Inorg. Chem.* **2002**, *41*, 5821. Liu, J.-C.; Guo, G.-C.; Huang, J.-S.; You, X.-Z. *Inorg. Chem.* **2003**, *42*, 235. Liu, X.; de Miranda, M. P.; McInnes, E. J. L.; Kilner, C. A.; Halcrow, M. A. *Dalton Trans.* **2004**, 59. Abedin, T. S. M.; Thompson, L. K.; Miller, D. O.; Krupicka, E. *Chem. Commun*. **2003**, 708.
(15) (a) Beckett, R.; Hoskins, B. F. *J. Chem. Soc., Dalton Trans.* **1972**, 291. (b) Butcher, R. J.; O'Connor, C. J.; Sinn, E. *Inorg. Chem.* **1981**, *20*, 537. (c) Baral, S.; Chakravorty, A. *Inorg. Chim. Acta* **1980**, *39*, 1.
(16) Angaroni, M.; Ardizzoia, G. A.; Beringhelli, T.; La Monica, G.; Gatteschi, D.; Masciocchi, N.; Moret, M. *J. Chem. Soc., Dalton Trans.* **1990**, 3305. Angaridis, P. A.; Baran, P.; Boca, R.; Cervantes-Lee, F.; Haase, W.; Mezei, G.; Raptis, R. G.; Werner, R. *Inorg. Chem.* **2002**, *41*, 2219.
(17) Schlemper, E. O. *Inorg. Chem.* **1968**, *7*, 1130.

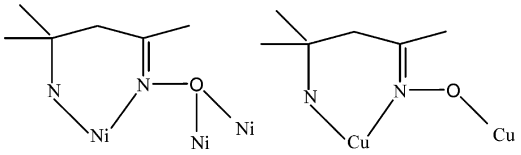

Figure 1. Schematic illustration of the coordination modes of $amox^-$ in complexes **1** and **2**.

Table 2. Selected Bond Distances (Å) and Angles (deg) for **1**[a]

Ni(1)−N(2)	2.014(4)	Ni(1)−O(1)	2.030(4)
Ni(1)−O(2)#1	2.142(3)	Ni(1)−O(2)#2	2.142(3)
Ni(1)−N(1)	2.070(5)	Ni(1)−O(3)	2.1267(14)
Ni(2)−N(4)	2.034(3)	Ni(2)−O(1)	2.042(3)
Ni(2)−N(3)	2.072(3)	Ni(2)−O(3)	2.1152(10)
Ni(2)−O(4)#1	2.115(3)	Ni(2)−O(2)#2	2.146(3)
N(4)−O(2)	1.394(4)	O(4)−N(2)	1.395(6)
Ni(1)···Ni(2)	2.7928(16)	Ni(2)···Ni(2)#3	2.767(2)

Ni(2)−O(3)−Ni(2)#2	98.28(5)	Ni(2)#3−O(3)−Ni(2)	81.72(5)
Ni(2)−O(3)−Ni(1)#1	97.65(5)	Ni(2)−O(3)−Ni(1)	82.35(5)
Ni(1)−O(1)−Ni(2)	86.61(11)	Ni(2)#3−O(1)−Ni(2)	85.34(15)
O(2)−N(4)−Ni(2)	112.5(2)	N(4)−O(2)−Ni(1)#1	107.78(19)
N(4)−O(2)−Ni(2)#2	109.0(2)	N(2)−O(4)−Ni(2)#2	108.2(2)
Ni(2)#1−O(4)−Ni(2)#2	81.71(14)	O(4)−N(2)−Ni(1)	113.2(3)

[a] #1 $-x, -y, -z + 1$; #2 $-x, y, -z + 1$; #3 $x, -y, z$.

Table 3. Selected Bond Distances (Å) and Angles (deg) for **2**

Cu(1)−O(7)	1.935(4)	Cu(1)−O(5)	1.972(4)
Cu(1)−N(5)	1.988(5)	Cu(1)−N(6)	1.993(5)
Cu(1)−Cl(2)	2.7324(19)	Cu(2)−N(13)	2.004(3)
Cu(1)−N(10)	2.011(3)	Cu(2)−N(4)	1.956(5)
Cu(2)−O(6)	1.920(4)	Cu(2)−O(5)	1.969(4)
Cu(2)−N(3)	1.983(5)	Cu(2)−Cl(2)	2.749(2)
Cu(3)−O(8)	1.911(4)	Cu(3)−N(1)	1.960(5)
Cu(3)−N(2)	1.966(5)	Cu(3)−O(5)	1.977(4)
Cu(3)−Cl(2)	2.814(2)	N(2)−O(6)	1.371(6)
O(7)−N(4)	1.378(6)	N(6)−O(8)	1.363(6)
Cu(1)···Cu(2)	3.151(1)	Cu(1)···Cu(3)	3.089(1)
Cu(3)···Cu(2)	3.092(1)		

O(8)−N(6)−Cu(1)	115.1(4)	N(6)−O(8)−Cu(3)	114.0(3)
N(4)−O(7)−Cu(1)	115.6(3)	O(7)−N(4)−Cu(2)	117.3(3)
N(2)−O(6)−Cu(2)	112.7(3)	O(6)−N(2)−Cu(3)	116.4(4)
Cu(1)−Cl(2)−Cu(2)	70.19(5)	Cu(1)−Cl(2)−Cu(3)	67.7(1)
Cu(3)−Cl(2)−Cu(2)	67.5(2)	Cu(2)−O(5)−Cu(1)	106.19(17)
Cu(1)−O(5)−Cu(3)	102.90(19)	Cu(2)−O(5)−Cu(3)	103.17(18)

respectively. Figure 1 illustrates the coordination modes of $amox^-$ in the two complexes.

X-ray crystallography of **1** reveals that it consists of a polynuclear $[Ni_6(amox)_6(\mu_6\text{-}O)(\mu_3\text{-}OH)_2]^{2+}$ cation (Figure 2) and two Cl^- anions as the counterions. The environment of the Ni^{II} ions is nearly identical: each is surrounded by two nitrogen atoms of an $amox^-$ ligand and four oxygen atoms of two bridging oxime groups, one μ_3-OH^-, and one μ_6-O^{2-}. Each $amox^-$ ligand chelates to one Ni^{2+} ion and at the same time bridges two other Ni^{2+} ions using the oxime oxygen atom (Figure 1). The central μ_6-O^{2-} octahedrally connects six Ni^{2+} ions with Ni−O bond distances of 2.126(1) and 2.115(1) Å, which are greatly shorter than that (av. 2.40(4) Å) for μ_6-Cl^-−Ni bond distances.[1b] The structure of this Ni_6O core is related to the Ni_6O core in a Ni_{10} cluster,[1c] Fe_6O,[18c,e,f] Ln_6O[18a,b] (Ln^{3+} = Nd, Gd, Yb), and polyoxoanion $M_6O_{19}^{2-}$ (M = Mo, W).[18d] The six Ni^{2+} ions arrange to form a novel cage-like cluster. The cage is much like the Chinese lantern with the centered μ_6-O^{2-} as the candle (Figure 3).

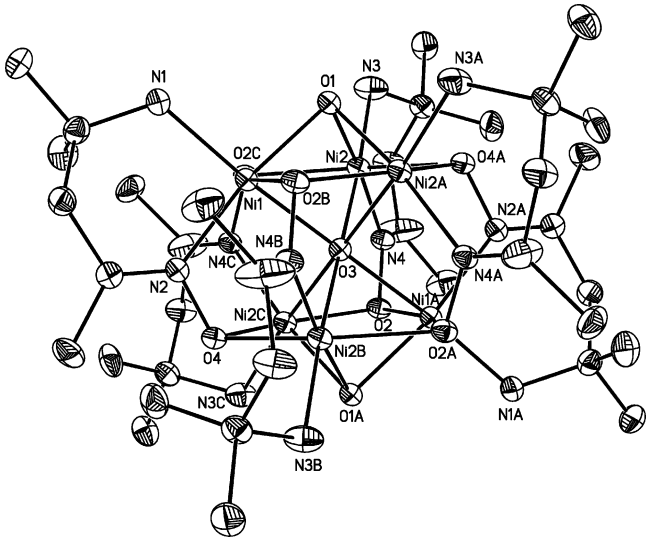

Figure 2. ORTEP plot of the hexanuclear $[Ni_6(amox)_6(\mu_6\text{-}O)(\mu_3\text{-}OH)_2]^{2+}$ cation in **1** drawn at 30% probability thermal ellipsoids (hydrogen atoms and water molecules are not shown for clarity).

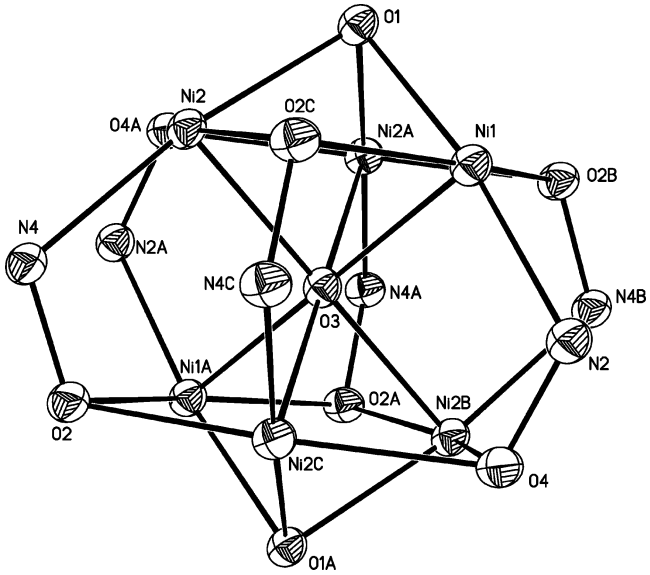

Figure 3. Chinese-lantern-like Ni_6 cage of **1**.

In the lantern-like Ni_6 cage each μ_3-OH^- links three Ni^{2+} ions with Ni···Ni separations of 2.767(2) and 2.792(2) Å. This results in the formation of two isosceles triangles at the top and bottom of the lantern. The top and bottom Ni(II) ions are further connected by the oxime ligands besides the μ_6-O^{2-} anion. The corresponding Ni···Ni distances are 3.199 and 3.193 Å, longer than that within two isosceles triangles. The Ni···Ni distances less than 2.70 Å have been observed in polynuclear Ni^{2+} complexes with planar or square pyramidal Ni^{2+} ions. To our knowledge, all the

(18) (a) Zhang, D.-S.; Ma, B.-Q.; Jin, T.-Z.; Gao, S.; Yan, C.-H.; Mak, T. C. W. *New J. Chem.* **2000**, *24*, 61. (b) Liu, J.; Meyers, E. A.; Shore, S. G. *Inorg. Chem.* **1998**, *37*, 5410. (c) Hegetschweiler, K.; Schmalle, H.; Streit, H. M.; Schneider, W. *Inorg. Chem.* **1990**, *29*, 3625. (d) Strong, J. B.; Ostrander, R.; Rheingold, A. L.; Maatta, E. A. *J. Am. Chem. Soc.* **1994**, *116*, 3601. (e) Caneschi, A.; Cornia, A.; Lippard, S. J.; Papaefthymiou, G. C.; Sessoli, R. *Inorg. Chim. Acta* **1996**, *243*, 295. (f) Cornia, A.; Gatteschi, D.; Hegetschweiler, K. *Inorg. Chem.* **1994**, *33*, 1559.

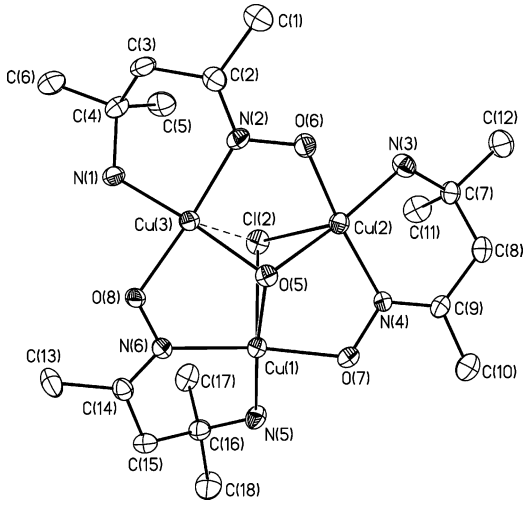

Figure 4. View of the ligand−metal environment in complex **2**. Hydrogen atoms and discrete anions are omitted for clarity.

reported Ni−Ni distances in the octahedral Ni^{2+} clusters are more than 2.80 Å. It is understandable that the six-coordinate Ni^{2+} ions are further apart than the four- or five-coordinate Ni^{2+} ions (2.21−2.54 Å)[19] on the basis of bond valence sum (BVS) analysis.

The structure of complex **2** consists of triangular cationic units, $[Cu_3(amox)_3(OH)Cl]^+$ (Figure 4), discrete ClO_4^- counteranions, and crystallization water molecules. The geometry of each copper(II) ion is best described as a distorted (4 + 1) (NN′OO′ + Cl) square-based pyramid. Similar to the previously reported Cu−amox complex,[11] each copper(II) ion is chelated by both the amine and oximato nitrogen atoms of one $amox^-$ ligand and the oxime oxygen atom of the adjacent $amox^-$ ligand, while a μ_3-OH^- completes square-planar tetracoordination of the three metal atoms with Cu−O bond distances of 1.972(4), 1.969(4), and 1.977(4) Å. Each $amox^-$ ligand chelates to one Cu^{2+} ion and at the same time links another Cu^{2+} ion using the oxime oxygen atom (Figure 1). Differently, a μ_3-Cl^- ion caps the opposite side of Cu_3 plane, occupying the apical position of square pyramidal coordination sphere of the three Cu(II) ions. The Cl−Cu bond distances range from 2.732(2) to 2.814(2) Å with two short and one long coordination bonds (Cu(1)−Cl(2) = 2.7324(19) Å, Cu(2)−Cl(2) = 2.749(2) Å, Cu(3)−Cl(2) = 2.814(2) Å). The four atoms that define each of the three basal planes around the Cu(II) ions deviate significantly from planarity except the coplanar O(5), O(7), N(5), and N(6) atoms around Cu(1). The copper atoms lie slightly out of the basal planes at distances of 0.1036, 0.0990, and 0.0823 Å toward the apical Cl(2) ion. Dihedral angels between the adjacent basal planes are 40.4° (Cu(1) plane−Cu(2) plane), 45.0° (Cu(1) plane−Cu(3) plane), and 46.5° (Cu(2) plane−Cu(3) plane). The Cu_3 cluster can be considered as an isosceles triangle with distances of 3.089 (Cu(1)···Cu(3)), 3.092 (Cu(2)···Cu(3)), and 3.151 Å (Cu(1)···Cu(2)). Chains are formed via hydrogen-bond interactions between OH^- and Cl^- ions of the adjacent Cu_3 clusters with a OH···Cl bond length of 2.113 Å and O−H···Cl angle of 171.6° (see Supporting Information).

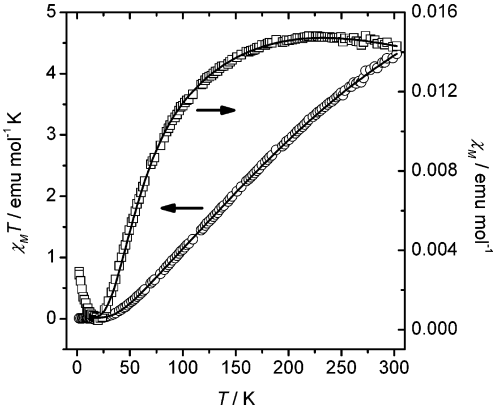

Figure 5. Temperature dependences of $\chi_M T$ (○) and χ_M (□) for **1**. Solid lines represent the best-fitting results (see text for *J* values obtained).

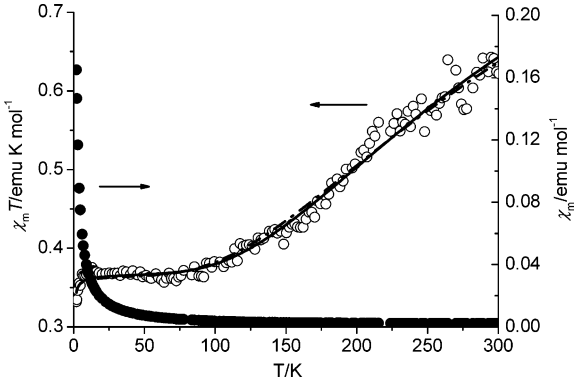

Figure 6. Temperature dependence of χ_MT (○) and χ_M (●) for **2**: dashed line, timer model with two *J* values; solid line, trimer with one *J*.

It can be seen that the structures of the two complexes are different, which is due to the different coordination properties of the two metal ions. The Cu(II) ion with a d^9 electron configuration is usually four- or five-coordinate due to the Jahn−Teller effect, which makes it impossible for the Cu(II) complex to possess a structure similar to that of the Ni(II) complex.

Magnetic Properties. Magnetic susceptibilities of **1** and **2** were measured in the temperature range 2−300 K on many manually selected single crystals. Figures 5 and 6 show the $\chi_M T$ vs *T* and χ_M vs *T* plots for **1** and **2**, respectively.

The $\chi_M T$ value for six Ni(II) ions at room temperature is 4.12 cm^3 mol^{-1} K, smaller than the typical value for six isolated Ni(II) ions (6 × 1.00 = 6 cm^3 mol^{-1} K) assuming $g = 2.0$ (which is unrealistic for a Ni(II) ion, which always has *g* values >2.00). Decreasing the temperature, $\chi_M T$ values decrease to 0 cm^3 mol^{-1} K at 2 K. The feature of this curve is indicative of strong antiferromagnetic coupling. A plot of χ_M corroborates this feature: the χ_M for six Ni(II) ions at room temperature is 0.0136 cm^3 mol^{-1}, there is then a slight increase to a maximum close to 250 K (0.014 cm^3 mol^{-1}), and then decrease smoothly to 0 cm^3 mol^{-1} at ca. 20 K. From 20 to 2 K there is a small increase, undoubtedly due to a small percentage of paramagnetic (assumed mononuclear)

(19) Sacconi, L.; Mealli, C.; Gatteschi, D. *Inorg. Chem.* **1974**, *13*, 1985. Shieh, S. J.; Chou, C. C.; Lee, G. H.; Wang, C. C.; Peng, S. M. *Angew. Chem., Int. Ed. Engl.* **1997**, *36*, 56. Berry, J. F.; Cotton, F. A.; Lu, T.; Murillo, C.; Wang, X. *Inorg. Chem.* **2003**, *42*, 3595.

Scheme 1. Three Possible Magnetic Pathways (J_1, J_2 and J_3) in Complex **1**

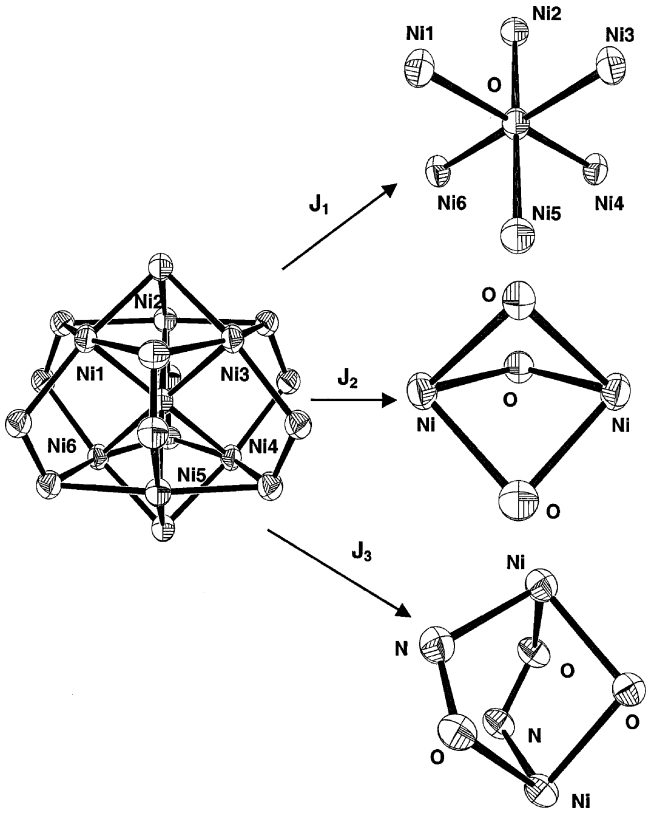

nickel impurities, always present when antiferromagnetic coupling is large.

To fit and interpret the magnetic susceptibility data of complex **1**, first it is necessary to find all possible magnetic pathways in the complicated but regular structure of complex **1**. Close examination of the structure gives the pathways shown in Scheme 1. From this scheme we deduce three different magnetic pathways and thus three different kinds of J values: the Ni−O−Ni entities placed in a trans position, named J_1; the Ni−O−Ni coupling within each triangle (upper and lower) through the oxo atoms of the ligands and the central oxo bridge, named J_2; and, finally, the J values between the upper or lower triangles through the central oxo bridge and the Ni−N−O−Ni of the oxime, named J_3. There are six J_2 and six different J_3 pathways. For the sake of simplicity, only one J_2 and J_3 are shown in Scheme 1. The other five are equivalent.

Such a complicated magnetic structure represents an interesting challenge in order to fit and interpret the susceptibility data. J_1 pathways seem to be the most defined. According to the literature data, this coupling must be strongly antiferromagnetic (AF). In effect, at the beginning of the molecular magnetism studies this M−O−M arrangement at 180° was presented as an ideal structure for strong antiferromagnetism. The known rules of Goodenough and Kanamori, derived from valence-bond theory, already represent this linearity as the origin of strong AF coupling.[20,21] Hoffmann and co-workers achieved the same results through more sophisticated MO calculations.[22] Logically, Kahn also explained this feature in his book.[23]

The same rules and calculations also state that when the M−O−M angle is 90° the coupling would be ferromagnetic (F). Thus, a first problem arises to interpret even the sign of J_2 and J_3 (Scheme 1). J_2 corresponds to the six Ni−O(3)−Ni pathways within the two upper and lower triangles. The three angles Ni−O−Ni are between 81−86°, indicating the possibility of antiferro- or ferromagnetic coupling. For J_3 the situation is also complicated: the two Ni−O−N−Ni pathways should be antiferromagnetic due to overlap between the magnetic orbital or the Ni(II) ions through the N and O p orbitals, but the nonplanarity of these Ni−O−N−Ni entities (noticeable dihedral angle) will reduce the antiferromagnetism, giving rise to small antiferromagnetic coupling. At the same time, the Ni ions are also linked through the central oxo bridge at ca. 87° that can give ferromagnetic coupling.[8,24]

Thus, several attempts have been made with magnetic data in order to draw the main magneto-structural data. In all cases a full diagonalization method by means of the Clumag program has been used to fit each possible situation.[25] Reasonable fits were only obtained assuming that J_1 is the dominant coupling and strongly antiferromagnetic. With this hypothesis the best-fit results are as follows: $J_1 = -150.4(2)$ cm^{-1}, $J_2 \approx 0$ cm^{-1}, $J_3 = -25.0(1)$ cm^{-1}, $g = 2.26$, and $R = 8.6 \times 10^{-7}$ ($R = \sum|(\chi_M T)_{obs} - (\chi_M T)_{calcd}|^2/\sum(\chi_M T)_{obs}^2$) assuming a molecular TIP of 600×10^{-6} emu mol^{-1}, according to the values given in the literature[23] (Figure 5). It is worth mentioning that the J_1 value is comparable with that for a structurally related Ni_{10} complex.[1c]

Thus, although such a case is impossible to solve perfectly due to its intrinsic limitations, we can conclude that J_1 is the dominant parameter, which gives the strong antiferromagnetic coupling, tuned by J_3. J_2 is, apparently, inconclusive. The magnitude of J_1 seems logical (very strong antiferromagnetic) owing to the Ni−O−Ni angle of 180°. J_3 is only ca. -25 cm^{-1}, probably due to the mixing of the two equivalent Ni−O−N−Ni distorted pathways (AF) and the Ni−O−Ni at 87° (F). The fit value of J_2 is likely a mathematical artifact. Simulations made keeping both the calculated values of J_1 and J_3 and changing J_2 from 0 to weakly positive (ferromagnetic) values do not vary the R value of the fit (always close to 10^{-6}). This feature (indetermination of J_2) can be interpreted as showing the topology of the spins in the global structure, assuming (in agreement with the experimental results) J_1 is strongly antiferromagnetic and J_3 is weakly antiferromagnetic (Figure 7). The three $S = 1$ spins are up (or down) in the upper triangle and, thus, down (or up) in the lower triangle. Within

(20) Goodenough, J. B. *Phys. Rev.* **1955**, *100*, 565; *J. Phys. Chem. Solids* **1958**, *6*, 287.
(21) Kanamori, J. *J. Phys. Chem. Solids* **1959**, *10*, 87.
(22) Hay, P. J.; Thibeault, J. C.; Hoffmann, R. *J. Am. Chem. Soc.* **1975**, *97*, 4884
(23) Kahn, O. *Molecular Magnetism*; VCH Publishers: New York, 1993.
(24) Paine, T. K.; Rentschler, E.; Weyhermuller, T.; Chaudhuri, P. *Eur. J. Inorg. Chem.* **2003**, 3167.
(25) Gatteschi, D.; Pardi, L. *Gazz. Chim. Ital.* **1993**, *123*, 231. The series of calculations were made using the computer program CLUMAG, which uses the irreducible tensor operator (ITO) formalism.

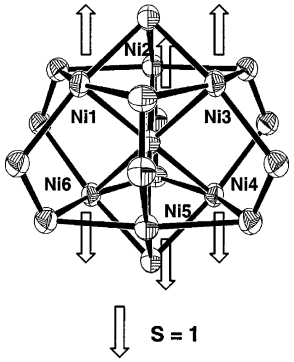

Figure 7. Spin topology for complex **1**, assuming J_1 is strongly AF, J_2 is negligible, and J_3 is weakly AF.

each triangle the $S = 1$ spins are *obliged* to be parallel, except in the case that it was the predominant magnetic pathway. Thus, it is not unexpected that the best fit gives a positive J_2 value (F) close to 0. A similar situation occurred in the Ni_{10} complex.[1c]

The gradual decrease of $\chi_M T$ values per Cu_3 with decreasing T for compound **2** clearly indicates the existence of an antiferromagnetic interaction. The $\chi_M T$ value is 0.622 cm^3 mol^{-1} K at 300 K, much lower than the value of 1.3 cm^3 mol^{-1} K expected for three uncoupled Cu(II) ions assuming $g = 2.0$. The $\chi_M T$ value plateaus at 0.36−0.37 cm^3 mol^{-1} K between 25 and 80 K before decreasing again at lower temperatures and reaches 0.33 cm^3 mol^{-1} K at 2 K. The plateau value corresponds well to that (0.375 cm^3 mol^{-1} K) for one Cu(II) ion with $S = 1/2$ ($g = 2.0$), and the further decrease below 25 K is due to the presence of intermolecular antiferromagnetic interaction.

A simpler trimer model with only one coupling parameter J is taken to fit the magnetic susceptibility data with the spin Hamiltonian[26] described in the following form: $\hat{H} = -2J(\hat{S}_1\hat{S}_2 + \hat{S}_2\hat{S}_3 + \hat{S}_1\hat{S}_3)$.

A closed-form solution of the magnetic susceptibility may be derived from this Hamiltonian in which Weiss-like parameter θ was considered to analyze the experimental variation $\chi_M T$ at low temperatures

$$\chi_M = \frac{Ng^2\beta^2}{4k(T-\theta)} \frac{1 + 5\exp(3J/kT)}{\exp(3J/kT) + 1}$$

The result of best fit, as shown (solid line) in Figure 6, is $J = -109(1)$ cm^{-1}, $g = 2.0$ (fixed), $\theta = -0.27(5)$ K, and $R = 7.1 \times 10^{-4}$ ($R = \sum|(\chi_M T)_{obs} - (\chi_M T)_{calcd}|^2/\sum(\chi_M T)_{obs}^2$).

According to the crystal structure of **2** the linkage between Cu(1) and Cu(3) ions through the oxime, μ_3-Cl^-, and μ_3-OH^- bridge is similar to the linkage between Cu(2) and Cu(3) ions. The exchange Hamiltonian of an isosceles triangular arrangement of three metals takes on the form $\hat{H} = -2J_1(\hat{S}_1\hat{S}_3 + \hat{S}_2\hat{S}_3) + 2J_2\hat{S}_1\hat{S}_2$ for the Cu_3 cluster, where J_1 refers to the interaction between Cu(3) and Cu(1) or Cu(2) and J_2 to the interaction between Cu(1) and Cu(2).[15−17,26] The corresponding molar magnetic susceptibility is expressed by the equation below. Assuming that the g values for all three copper atoms are equal, the following equation applies

$$\chi_M = \frac{Ng^2\beta^2}{4k(T-\theta)} \frac{10\exp(J_1/kT) + \exp(-2J_1/kT) + \exp(-2J_2/kT)}{2\exp(J_1/kT) + \exp(-2J_1/kT) + \exp(-2J_2/kT)}$$

The least-squares fitting to the susceptibility data yields the following parameters: $J_1 = -60(8)$ cm^{-1}, $J_2 = -170(8)$ cm^{-1}, $g = 2.0$ (fixed), $\theta = -0.26(4)$ K, and $R = 6.3 \times 10^{-4}$ ($R = \sum|(\chi_M T)_{obs} - (\chi_M T)_{calcd}|^2/\sum(\chi_M T)_{obs}^2$), as shown in Figure 6 (dashed line).

Both fittings, from a mathematical point of view, are rational. The latter method gets a smaller residual error and the J_1 and J_2 values obtained significantly differ from those obtained with only one J value. Moreover, the ratio of J_2/J_1 is far away from 1. It is believed that the isosceles triangle model, which better accords with the structure, is more suitable to explain the magnetic properties.

A considerable amount of literature work has established relationships between the magnetic coupling and certain structural features for the trinuclear copper(II) complexes.[14−17] It has been well documented that the more flattened the $Cu_3O(H)$ bridge, the stronger the magnetic interaction, and higher coplanarity of the coordination planes around each copper atom is followed by a larger spin coupling constant.[15] For this work, on one hand, O(H) is 0.816 Å out of the Cu_3 plane, due to μ_3-Cl^- occupying the opposite side, which implies a smaller J value. On the other hand, the dihedral angle of 40.4° between equatorial planes of Cu(1) and Cu(2) atoms is smaller than the dihedral angles of 45.0° and 46.5° between the equatorial planes of Cu(1) and Cu(3) and Cu(2) and Cu(3), respectively. The closer this dihedral angle is to 0°, the larger the magnetic orbital $d_{x^2-y^2}$ overlaps and the stronger the magnetic exchange interaction. The fitting result that J_2 of $-170(8)$ cm^{-1} is much more negative than the J_1 value of $-60(8)$ cm^{-1} is consistent with this rule. The highest coplanarity was reported for the oxime compound $[Cu_3(\mu_3\text{-}O)L_3(ClO_4)]_2$ [HL = 1,2-diphenyl-2-(methylimino)-ethanone-1-oxime],[16b] with an averaged interplanar angle of 20.3°, with a J constant of -2000 cm^{-1}. The related compound $[Cu_3(\mu_3\text{-}OH)L'_3(ClO_4)](ClO_4)$ [HL′=3-(phenylimino)-butanone-2-oxime], with an average interplanar angle of 33°, exhibits a J constant of -244 cm^{-1}.[16b] Compound **2** with an average interplanar angle of 43° exhibits rational smaller J constant. The small θ value of $-0.16(5)$ K indicates that the intramolecular interactions via H bonds contribute little to the magnetic coupling.

Conclusions

Complex **1** is the first structurally characterized oxime-bridged Ni_6 complex with shortest octahedral $Ni^{II}\cdots Ni^{II}$

(26) Sinn, E.; Harris, C. M. *Coord. Chem. Rev.* **1969**, *4*, 391.

contacts. The six Ni^{2+} ions form a cage encapsulating a rare μ_6-Oxo anion. Strong short-range Ni^{II}−Ni^{II} antiferromagnetic coupling has been observed and analyzed. Complex **2** has a rare structure of an oxime-bridged Cu_3 triangle capped by both μ_3-OH^- and μ_3-Cl^- ions. Future work will be devoted to the synthesis of $amox^-$- and modified $amox^-$-based $Mn^{II/III}$ species that might exhibit SMM (single-molecule magnet) behavior.

Acknowledgment. This work was supported by the National Natural Science Foundation of China (Projects 20201008 and 50272034).

Supporting Information Available: Cell packing diagrams for **1** and **2**; plot showing the intermolecular interaction for complex **2**; X-ray crystallographic file (CIF). This material is available free of charge via the Internet at http://pubs.acs.org.

IC048729M